The histone demethylase Kdm3a is essential to progression through differentiation

Marielle Herzog, Eléonore Josseaux, Sarah Dedeurwaerder, Emilie Calonne, Michael Volkmar and François Fuks*

Laboratory of Cancer Epigenetics, Faculty of Medicine, Université Libre de Bruxelles, 808 route de Lennik, 1070 Brussels, Belgium

ABSTRACT

Histone demethylation has important roles in regulating gene expression and forms part of the epigenetic memory system that regulates cell fate and identity by still poorly understood mechanisms. Here, we examined the role of histone demethylase Kdm3a during cell differentiation, showing that Kdm3a is essential for differentiation into parietal endoderm-like (PE) cells in the F9 mouse embryonal carcinoma model. We identified a number of target genes regulated by Kdm3a during endoderm differentiation; among the most dysregulated were the three developmental master regulators *Dab2, Pdlim4* and *FoxQ1*. We show that dysregulation of the expression of these genes correlates with Kdm3a H3K9me2 demethylase activity. We further demonstrate that either *Dab2* depletion or *Kdm3a* depletion prevents F9 cells from fully differentiating into PE cells, but that ectopic expression of *Dab2* cannot compensate for *Kdm3a* knockdown; *Dab2* is thus necessary, but insufficient on its own, to promote complete terminal differentiation. We conclude that Kdm3a plays a crucial role in progression through PE differentiation by regulating expression of a set of endoderm differentiation master genes. The emergence of Kdm3a as a key modulator of cell fate decision strengthens the view that histone demethylases are essential to cell differentiation.

INTRODUCTION

Tight control of the gene expression program is crucial for developing organisms. During development, decisions are made between self-renewal and differentiation, and specific gene expression patterns are established. These choices result in a complex interplay of different pathways. In recent years, epigenetic mechanisms, which regulate chromatin structure, have emerged alongside the transcription factor network as key regulators of the balance between pluripotency and lineage-specific differentiation (1,2).

Post-translational modifications of histones, including phosphorylation, ubiquitylation, acetylation and methylation, are important epigenetic modifications with pivotal roles in chromatin regulation. The histone methylation pattern of a gene determines whether it is transcriptionally active or inactive. In general, trimethylation of H3K4, H3K36 and H3K79 (to H3K4me3, H3K36me3, H3K79me3, respectively) correlates with an active gene status, whereas di- and trimethylation of H3K9 (to H3K9me2/me3) and trimethylation of H4K20 and H3K27 (to H4K20me3 and H3K27me3) is associated with transcriptional repression. The level and distribution of histone methylation are involved in controlling numerous biological processes including maintenance, self-renewal and pluripotency on the one hand and differentiation on the other (3–6). Until a few years ago, histone methylation was regarded as an irreversible modification. The identification of a first histone demethylase, Kdm1a (7) and thereafter of a second family of histone demethylases, the JmjC-domain-containing proteins (8), provided compelling evidence of a more dynamic regulation of the methylation state of histones. By now, several classes of histone demethylases have been discovered, differing in their specificities with regard to target lysine residues and the degree of methylation. Functional studies have implicated specific demethylases in controlling gene expression programs and cell fate decisions, supporting the emerging idea that histone demethylases are key players in developmental

processes (9). Although investigators are beginning to understand some biological roles of histone demethylases, much remains to be learned about the exact functions of these enzymes. H3K9 methylation is a well-characterized modification in eukaryotic chromatin, associated with transcriptional repression. In general, H3K9me3 is present in the heterochromatin compartment, while H3K9me2 occurs predominantly in euchromatin, where it is thought to have major functions in transcriptional control (10). In addition, euchromatic H3K9 dimethylation, regulated by the histone methyltransferase G9a, is described as a key component of mechanisms regulating gene expression during early embryonic development and differentiation (11). H3K9 is believed to be maintained in a demethylated state by two different families of JmjC-domain demethylases: Kdm4-family proteins catalyse the removal of di- and trimethylation, whereas Kdm3a removes mono- and dimethylation (12–14). Dynamic changes in H3K9 methylation have been observed at regulated, inducible inflammatory genes, suggesting that euchromatic H3K9 methylation could be a regulatory level in transcriptional activation (15). Yet, the role of dynamic control of H3K9 dimethylation in the earliest phases of development and differentiation is not yet well characterized. We are particularly interested in the H3K9me2-specific demethylase Kdm3a (14), shown in experiments with *Kdm3a* knockout mice to play an important role in germ cell development and metabolism (16,17). In addition, cell culture studies have linked Kdm3a to the regulation of androgen-receptor-dependent gene expression, hypoxia-inducible gene expression and (in collaboration with the H3K9me3 demethylase Kdm4c) self-renewal (14,18,19).

Here, in order to assess the importance of Kdm3a in cell fate decisions during early development, we have used F9 mouse embryonal carcinoma cells, a well-established model, to study crucial events in early differentiation (Figure 1A) (20). F9 cells markedly resemble the inner cell mass cells of the blastocyst embryo (3.5 days of gestation, E3.5), i.e. embryonic stem (ES) cells that can be induced to differentiate into primitive endoderm-like (PrE) cells upon treatment with retinoic acid (RA) and to progress through terminal differentiation into parietal endoderm-like (PE) cells after treatment with RA plus cyclic AMP (cAMP) (henceforth referred to as RA + dbcAMP) (21,22).

In this model, we have reduced the expression of *Kdm3a* with interfering RNAs, examined how *Kdm3a* depletion affects early and later stages of F9-cell differentiation, and identified genes whose expression is regulated by Kdm3a. We have found that *Kdm3a* depletion prevents F9 cells from fully differentiating into PE cells and that it causes dysregulation of master players in the differentiation process. Our results thus demonstrate, for the first time, a crucial role for Kdm3a in regulating terminal endodermal differentiation, highlighting the importance of demethylases in the fine-tuning of transcription during differentiation.

MATERIALS AND METHODS

F9 cell culture and transfection

Mouse embryonal carcinoma F9 cells were purchased from the American Type Culture Collection (ATCC) and grown as a monolayer on 0.1% gelatine-coated tissue culture dishes in Dulbecco's modified Eagle's medium (DMEM, Gibco) supplemented with 10% foetal bovine serum in 5% CO_2 at 37°C. To induce differentiation to PrE cells, F9 cells were treated with 1 μM all-*trans* RA (Sigma) for 3 days. To further induce differentiation to PE cells, F9 cells were treated with 1 μM RA in combination with 250 μM dibutyryl cAMP (dbcAMP, Sigma) for the indicated times, with a medium change every 2 days. When the differentiation time course was studied, the number of plated F9 cells was 5×10^6 in the case of no treatment, 3.5×10^5 cells for a 3-day of treatment and 1×10^5 cells for a 6-day treatment.

RNAi and retroviral infection

Short hairpin (sh) oligos targeting specific 20-bp regions were designed with the help of the Ambion siRNA database website. The sequences used to silence *Kdm3a* or *Dab2* were inserted into the pSuperRetro (pRS) retroviral vector according to the manufacturer's (OligoEngine) recommendations. Briefly, the retrovirus was produced by 293GP cells. After 24 h of production, virus-containing medium was collected and used to infect F9 cells. Starting 24 h after infection, infected F9 cells were selected with 1 μg/ml puromycin (Sigma). Oligonucleotide sequences for construction of the knockdown constructs are listed in Supplementary Table S2 (panel shRNA).

RNA extraction and qRT-PCR

Total RNA was extracted with TriPure™ reagent (Roche) and DNase treatment was performed with the DNA-free DNase kit (Ambion) according to the manufacturer's instructions. mRNA was reverse-transcribed into cDNA from 1.5 μg total RNA with the help of oligo-dT primers and SuperScript II™ reverse transcriptase (Invitrogen) according to the manufacturer's protocol and then used as template for real-time quantitative PCR based on SybrGreen detection with the Light Cycler 480 (LC480) system (Roche). Levels of target genes' cDNAs were measured by the comparative Ct method (ddCt method; Ct: threshold cycle number). The housekeeping gene *HPRT* was used as an internal control for normalization. The relative expression levels from at least triplicate experiments were averaged and expressed as means ± standard error (SEM). The PCR primers used for amplification are listed in Supplementary Table S2.

### Gene expression microarrays

Gene expression profiling was performed in two independent differentiation experiments. Total RNA from RNAi control and RNAi *Kdm3a* cells was isolated by the TriPure method (Roche) according to the manufacturer's instructions and purified on RNeasy minicolumns (Qiagen). The purity of the RNA obtained was assessed by spectrophotometry (OD 260 nm / OD 280 nm > 1.8). Total RNA
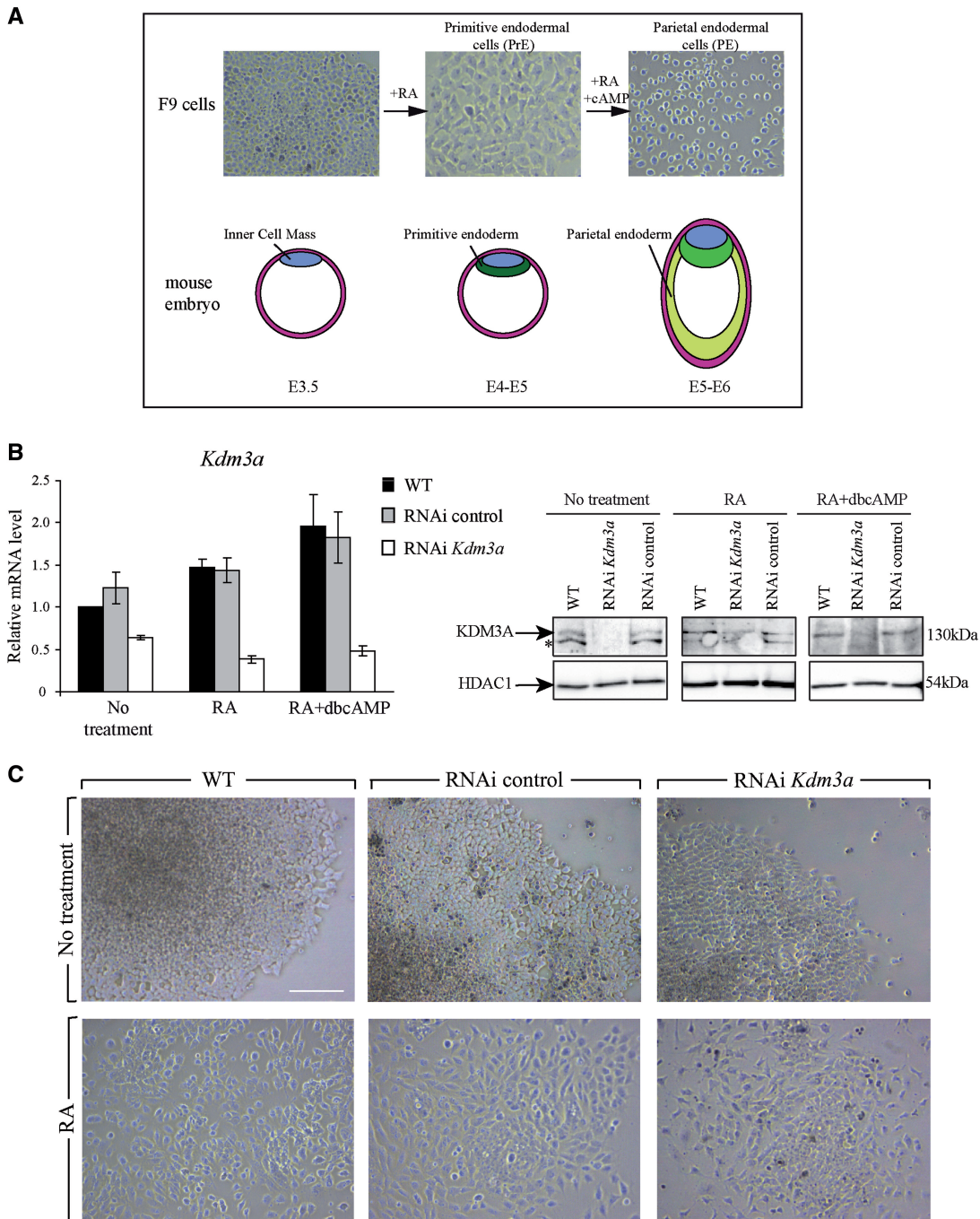
Figure 1. Kdm3a is required neither for maintenance of F9 cells in an undifferentiated state nor for PrE differentiation. (**A**) F9 mouse embryonal cell differentiation (top panels) in relation to normal early mouse embryogenesis (lower panels). At 3.5 days of gestation (E3.5), before implantation, the mouse embryo is at the blastocyst stage. The inner cell mass (ICM), which will become the embryo plus some extra-embryonic tissues, is established. Then, some ES cells at the surface of the ICM will become the primitive endoderm (E4–5); the remaining cells will form the embryo. In the first two days post-implantation, the primitive endoderm migrates to form the parietal endoderm (E5–6). The top panels show the morphology of F9 cells during their differentiation into PrE cells when grown in monolayer in the presence of RA. Addition of cAMP allows their differentiation into PE cells. (**B**) Quantitative RT-PCR analysis of *Kdm3a* expression and western blot analysis of the Kdm3a protein level after RNAi-mediated knockdown. F9 cells were infected with the empty pRS vector (RNAi control) or the *Kdm3a*-targeting pRS vector (RNAi *Kdm3a*). After selection, the RNAi control, RNAi *Kdm3a* and wild-type (WT) F9 cells were either left untreated (no treatment), cultured with RA for 3 days (RA), or cultured with RA for 3 days and then for 3 additional days with RA plus dbcAMP (RA+dbcAMP). Isolated RNA from these cells was subjected to qRT-PCR analysis with *Kdm3a*-specific primers. All transcript levels were normalized to *Hprt* and then normalized to the expression level recorded for untreated WT cells. Data are presented as means ± SEM (*n* = 4). Western blot analysis with antibody against Kdm3a showed a decreased level of this protein in RNAi *Kdm3a* cells as compared to control cells (WT and RNAi control) at all stages of the F9-cell differentiation process. The asterisk indicates a non-specific band detected with the anti-Kdm3a antibody. Hdac1 was used as a loading control. (**C**) RNAi *Kdm3a* cells differentiate into PrE cells. WT, RNAi control and RNAi *Kdm3a* cells treated or not with RA for 3 days were photographed under a phase contrast microscope. At the undifferentiated (top panels) and PrE (lower panels) stages, morphological analysis did not reveal any morphological defects in the RNAi *Kdm3a* cells as compared to WT or RNAi control cells. Bar = 200 µm.
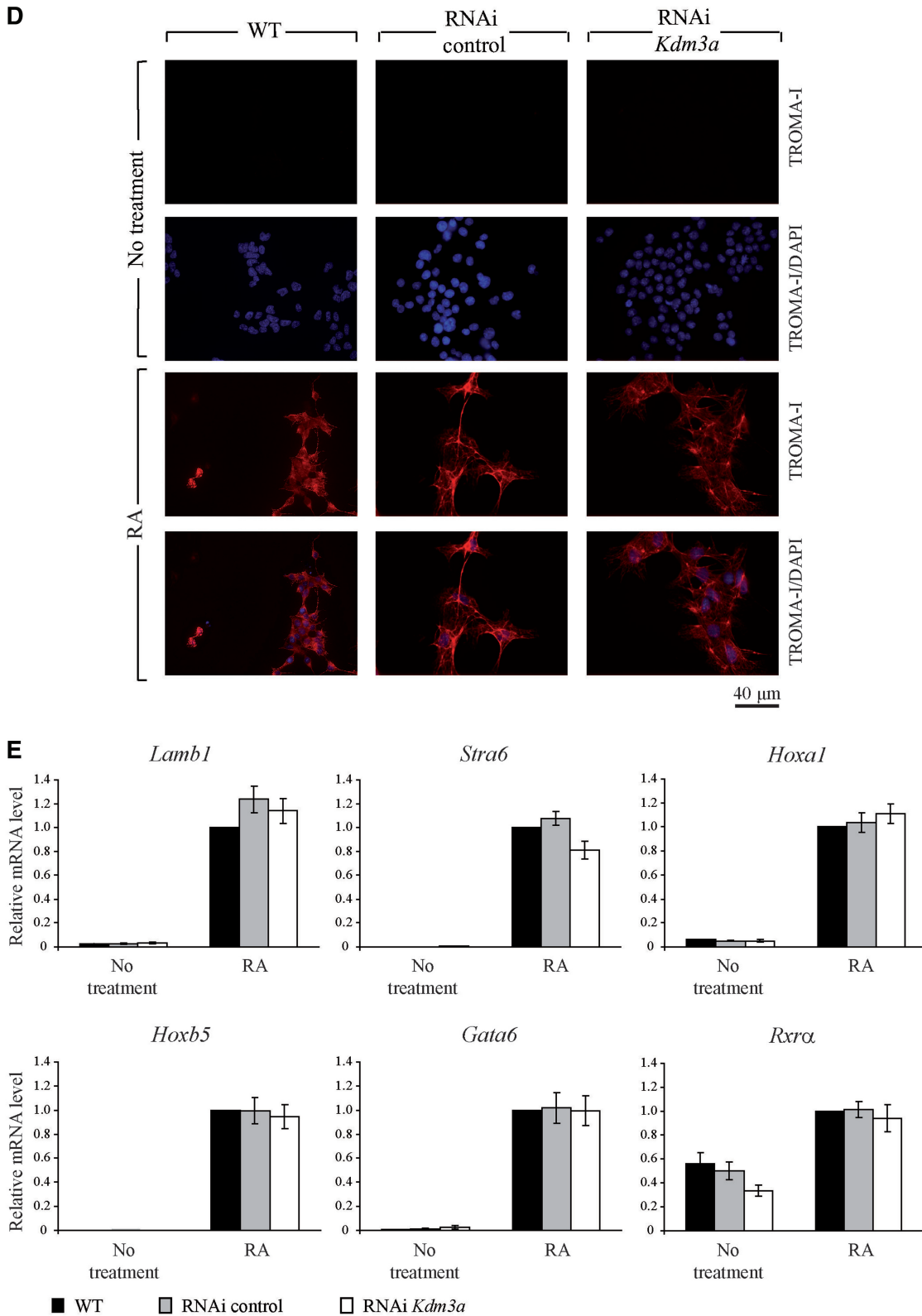
(continued)

Figure 1. Continued
(**D**) Normal expression of TROMA-1 in WT, RNAi control and RNAi *Kdm3a* F9 cells. Cells were cultured for 3 days with or without RA and then hybridized with an anti-TROMA-1 mAb. Cytoplasmic TROMA-1 staining was unaffected by *Kdm3a*-knockdown. Cell DNA content was visualized by DAPI staining. Bar = 40 μm. (**E**) Similar expression profiles of PrE-associated genes in WT, RNAi control and RNAi *Kdm3a* F9 cells treated or not with RA for 3 days. Relative expression of the *LamB1*, *Stra6*, *Hoxa1*, *Hoxb5*, *Gata6* and *Rxrα* genes was analysed by qRT-PCR. *Hprt* was used as an internal control. All transcript levels were corrected by the normalized level recorded for RA-treated WT cells. Values are represented as means ± SEM (*n* = 4).

(200 ng) was amplified with the Illumina® TotalPrep RNA Amplification Kit (Ambion) and then hybridized with the MouseWG-6 v2 array according to the Whole-Genome Gene Expression Direct Hybridization Assay (Illumina). Chips were scanned with the HiScan Reader (Illumina). Quality of the microarray data was checked with the 'beadarray' package of the R statistical software (http://www.r-project.org/) and data were normalized by the 'quantile' method. Finally, differential expression analyses were performed with the 'limma' package in R. For graphical representation as a heatmap, $\log_2$-transformed expression differences were used and visualized with the 'heatmap.2' function of the 'gplots' package of R. Supplementary Table S1 shows a summary of the analysed data, and all raw microarray data from our analyses have been deposited in the Gene Expression Omnibus (GEO) database under accession number GSE33841.

ChIP assay

ChIP assays were performed on F9 cells according to the protocol for the Diagenode LowCell# ChIP kit protein A (containing DiaMag protein A-coated magnetic beads). Sonication with a bioruptor (Diagenode) was optimized for 10^6 PE-differentiated F9 cells to obtain chromatin fragments with an average size of 500 bp. Then, 1/10 of the sheared chromatin was immunoprecipitated with 2 μg of either anti-H3K9me3 (Diagenode, pAb-056-050) or anti-H3K9me2 (Abcam, ab1220) antibody. No antibody was used in mock ChIP controls. Quantitative analysis was performed by real-time qPCR with the LC480 system (Roche) with 2 μl DNA and SybrGreen master mix and the primers listed in Supplementary Table S2. Ct values were determined for both immunoprecipitated DNA and a known amount of DNA from the input sample for the different primer pairs. The amount of immunoprecipitated chromatin corresponding to a particular genomic locus was then calculated from the qPCR data and reported as fold enrichment relative to the background (no antibody). The fold enrichment of immunoprecipitated DNA over background (no antibody) was calculated, as previously described (23,24), according to the delta-delta Ct method (ddCt), using the formula $2^{(-ddCt)}$, where $dCt = [Ct^{IP} - (Ct^{input} - 6.644)]$ (subtraction of 6.644, the $\log_2$ of 100, corrects for the use of 1% input material in the qPCR determining the C^{tinput}) and ddCt is the correction of the IP signal for background (no antibody). All fold enrichment values are means of three independent experiments.

Immunofluorescence

Cells were grown on gelatinized glass cover slips, washed with phosphate-buffered saline (PBS) and fixed with 2% paraformaldehyde for 10 min at room temperature. Samples were permeabilized twice with PBS containing 0.1% (w/v) Triton X100 (PBST) for 5 min at room temperature and washed with PBS. The cells were then incubated with primary antibody TROMA-1 (DSHB, diluted 1:10 in PBS) for 15 h at room temperature.

Samples were rinsed in PBST (2 times for 5 min) and incubated for 1 h at room temperature with Cy3-conjugated anti-mouse IgG secondary antibodies (Jackson Laboratories) diluted 1/500 in PBST, washed in PBST (2 × 5 min). Cells were stained for DNA with DAPI at 10 μg/ml. and mounted in a Vectashield® mounting medium (Vector Labs). Acquisition was done with a Leica DM3000 fluorescence microscope (Leica Microsystems).

Western blot analysis

Nuclear extracts of F9 cells were prepared and western blotting was carried out as described previously (25). Antibodies against Kdm3a (Santa Cruz; sc 107656) and HDAC1 (Diagenode, pAb 053-050) were used. Bound primary antibodies were visualized by chemoluminescence detection of HRP-labelled secondary antibodies (GE Healthcare), with the ECL detection kit (Perkin-Elmer) and a CCD camera system.

Dab2 rescue experiments

Dab2 cDNA was subcloned from a commercially available clone (Origene, MC200502) into pcDNA3.1-HA (CMV promoter). RNAi *Kdm3a* cells were transiently transfected using Lipofectamine reagent (Invitrogen) at a 1:5 ratio according to the manufacturer's instructions. Transfections were performed at the time points indicated during the F9 cell differentiation protocol (Figure 5A). *Dab2* over-expression was initially tested under different conditions, 48 h post-transfection, by qRT-PCR (data not shown). In the differentiation experiments, *Dab2* expression was analysed by qRT-PCR at the end of the differentiation protocol (*cf*. Figure 5; for PCR primer sequences, *cf*. Supplementary Table S2).

RESULTS

Kdm3a depletion allows normal PrE differentiation

To study the role of the H3K9me2 demethylase Kdm3a in regulating endodermal differentiation, we generated *Kdm3a*-knockdown F9 cells (RNAi *Kdm3a* cells), using a retroviral-vector-based short hairpin RNA (shRNA) approach (26). As controls we used both wild-type cells and cells infected with an empty vector (RNAi control cells). RNAi *Kdm3a* cells showed a significantly lower level of *Kdm3a* expression than either wild-type or RNAi control cells throughout the process of F9 cell differentiation, as demonstrated by quantitative reverse-transcription PCR (qRT-PCR) analysis and western blotting (Figure 1B and Supplementary Figure S1B). No obvious morphological difference was observed between untreated wild-type, RNAi control and RNAi *Kdm3a* cells, suggesting that Kdm3a does not play a crucial role in maintaining F9 cells in an undifferentiated state (Figure 1C, upper panel). To check the specificity of the effects of *Kdm3a* knockdown, we used a second shRNA against *Kdm3a*, giving rise to a similar knockdown efficiency and mirroring the knockdown effects and

phenotype obtained with the first shRNA targeting *Kdm3a* (Supplementary Figure S1).

We next wondered if *Kdm3a* depletion might affect the ability of F9 cells to differentiate. To answer this question, we first treated wild-type, RNAi control and RNAi *Kdm3a* cells for 3 days with 1 µM RA to promote differentiation to the primitive endoderm stage (PrE, *cf.* Introduction and Figure 1A). After RA treatment, the morphological changes characteristic of PrE differentiation, i.e. enlargement and a flat triangular morphology, appeared in all three cell populations (Figure 1C, lower panel and Supplementary Figure S1A). To confirm the PrE identity of these cells, we used immunocytochemistry in wild-type, RNAi control and RNAi *Kdm3a* cells cultured in the presence and absence of RA, to detect TROMA-1, a specific marker of endodermal F9-cell differentiation (27,28). The untreated wild-type, RNAi control and RNAi *Kdm3a* cells were found not to express TROMA-1 (Figure 1D), in contrast to all three populations of RA-treated cells (Figure 1D). The latter thus displayed both the morphological features and a molecular marker of PrE cells. To further investigate the response of RNAi *Kdm3a* cells to RA, we used qRT-PCR to analyse the transcript-level expression of different genes: (1) genes whose expression is known to be induced by RA treatment in F9 cells (genes encoding components of the extracellular matrix laminin B1 (*Lamb1*) (29), the transcription factor genes *Stra6, Hoxa1, Hoxb5, Rxrα* (30,31), and (2) the *Gata6* gene, shown to be important for mouse endoderm differentiation (32). As expected, all these genes turned out to be weakly or not expressed in the untreated wild-type, RNAi control and RNAi *Kdm3a* cells (Figure 1E and Supplementary Figure S1C). In contrast, all three cell populations showed similar induction of these genes after treatment with RA for 3 days (Figure 1E and Supplementary Figure S1C). Altogether, these results indicate that *Kdm3a*-knockdown cells can differentiate into PrE cells and hence, that the histone demethylase Kdm3a is not required for PrE differentiation.

Kdm3a is a crucial regulator of terminal F9-cell differentiation

Next, we examined the ability of wild-type, RNAi control and RNAi *Kdm3a* cells to further differentiate into PE cells. As mentioned in the introduction, the cells were stimulated to differentiate terminally by treatment for 3 days with 1 µM RA (for PrE) and then for 3 more days with 1 µM RA plus 250 µM dbcAMP (RA + dbcAMP). Under these conditions, the wild-type and RNAi control cells were found to differentiate into cells displaying the main features of PE cells: a rounded, refractive appearance with numerous long filopodia (Figure 2A). In contrast, most of the RNAi *Kdm3a* cells retained their PrE-like morphology (i.e. enlargement and a flat triangular morphology; Figure 2A and Supplementary Figure S1A). Analysis of TROMA-1 expression in RA + dbcAMP-treated RNAi *Kdm3a* cells confirmed their PrE differentiation stage (Figure 2B): the marker was still detected in the cytoplasm of most (but not all)

RNAi *Kdm3a* cells, but no longer in the cytoplasm of wild-type or RNAi control cells (Figure 2B). To analyse, at the molecular level, the response of RNAi *Kdm3a* cells to RA + dbcAMP treatment, we used qRT-PCR to measure transcript-level expression of the *Thrombomodulin* (TM) gene, a unique marker of PE differentiation (33). No TM expression was detected in untreated cells and only low expression in RA-treated cells, whether *Kdm3a* expression was knocked down or not (Figure 2C and Supplementary Figure S1D). After RA + dbcAMP treatment, both controls showed induced TM expression (Figure 2C and Supplementary Figure S1D), whereas RNAi *Kdm3a* cells showed drastically reduced induction (Figure 2C and Supplementary Figure S1D).

To determine if differentiation into PE cells might be delayed, rather than blocked, by *Kdm3a* knockdown, we cultured RNAi *Kdm3a* cells in the presence of both RA + dbcAMP for 6, 8 and 10 days (Supplementary Figure S2A). None of these treatments enabled RNAi *Kdm3a* cells to fully differentiate into PE cells, suggesting that PE differentiation was indeed blocked in these cells. Next, to see how specifically this effect was linked to *Kdm3a* depletion, we knocked down another H3K9 histone demethylase, Kdm4a, specific for H3K9me3/me2 demethylation. *Kdm4a* depletion in F9 cells did not cause any morphological anomaly during differentiation, suggesting that the phenotype observed in RNAi *Kdm3a* cells is related to the H3K9me2/me1 demethylase Kdm3a (Supplementary Figure 2B).

Taken together, our results demonstrate that most *Kdm3a*-knockdown cells remain blocked at the PrE stage and are unable to achieve terminal differentiation to the PE stage. Kdm3a is thus indispensable to the terminal differentiation of F9 cells into PE cells.

Kdm3a is essential for the induction of several differentiation genes

To better understand the role of Kdm3a in F9 cell differentiation, we used Illumina's MouseWG-6 v2.0 Expression BeadChip for expression profiling to identify potential downstream target genes of Kdm3a. We analysed gene expression in RNAi control and RNAi *Kdm3a* cells at different times during the differentiation process. Cells were either untreated and harvested on the day treatment started in the other cultures, or treated with 1 µM RA for 3 days, or treated first with 1 µM RA for 3 days and then for 3 extra days with 1 µM RA and 250 µM dbcAMP (RA + dbcAMP). Before microarray data analysis, we assessed the reproducibility of the microarray data and the robustness of the observed RA- and RA + dbcAMP-induced gene expression changes. For this, we generated a correlation matrix of all microarray-based unfiltered gene expression profiles (Pearson product–moment correlation; Supplementary Figure S3). The correlation coefficients were always highest between the two datasets for the same condition and generally lower between profiles corresponding to different conditions, indicating high reproducibility of the microarray data sets. As we profiled biological duplicates from independent differentiation experiments for gene
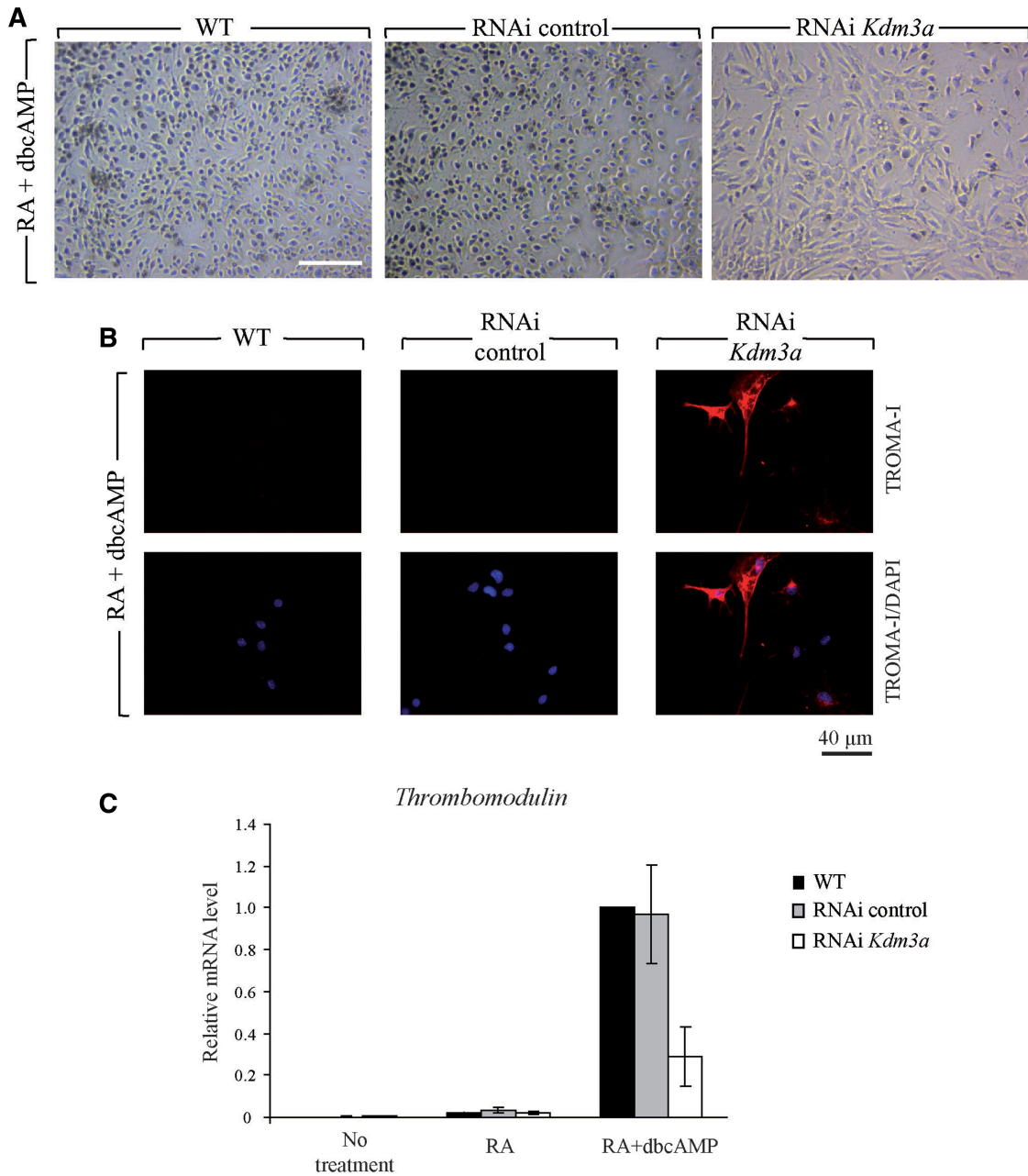
Figure 2. Kdm3a is required for terminal differentiation into PE cells. (**A**) Abnormal PE differentiation of RNAi *Kdm3a* F9 cells. WT, RNAi control and RNAi *Kdm3a* F9 cells were treated with RA for 3 days, then for 3 additional days with RA and dbcAMP (RA+dbcAMP) and photographed under a phase contrast microscope. WT and RNAi control cells show parietal endoderm morphology, whereas RNAi *Kdm3a* cells keep a PrE morphology. Bar = 200 μm. (**B**) TROMA-1 is still expressed in RNAi *Kdm3a* F9 cells after RA+dbcAMP. TROMA-1 was analysed by immuno-fluorescence in WT, RNAi control and RNAi *Kdm3a* F9 cells after 6 days of treatment. PE-differentiated WT and RNAi control cells show no TROMA-1 staining, but the stain is still present on RNAi *Kdm3a* cells indicating failure to differentiate into PE cells. The cell DNA content was visualized by DAPI staining. Bar = 40 μm. (**C**) Significant downregulation of expression of the PE differentiation marker *Thrombomodulin* (TM) in RNAi *Kdm3a* F9 cells. Cells were either not treated (no treatment), treated for 3 days with RA (RA), or treated for 3 days with RA and then for 3 additional days with RA and dbcAMP (RA+dbcAMP). Their mRNA was subjected to qRT-PCR with TM-specific primers. *Hprt* was used as an internal control. All transcript levels were substracted by the normalized level recorded for (RA+dbcAMP)-treated WT cells. Values are represented as means ± SEM (*n* = 3).

expression, the very high reproducibility of the microarray data further suggests good robustness for the transcriptional responses of F9 cells to the differentiation protocol.

In our microarray analysis performed on untreated cells, only three genes showed statistically significant dysregulation in RNAi *Kdm3a* cells: *Ccdc56*, *Krt17* and *Ccnd1*. This strengthens the view, based on cell morphology, that Kdm3a does not play a crucial regulatory role in undifferentiated F9 cells (Figure 3A and Supplementary Table S1). After RA+dbcAMP
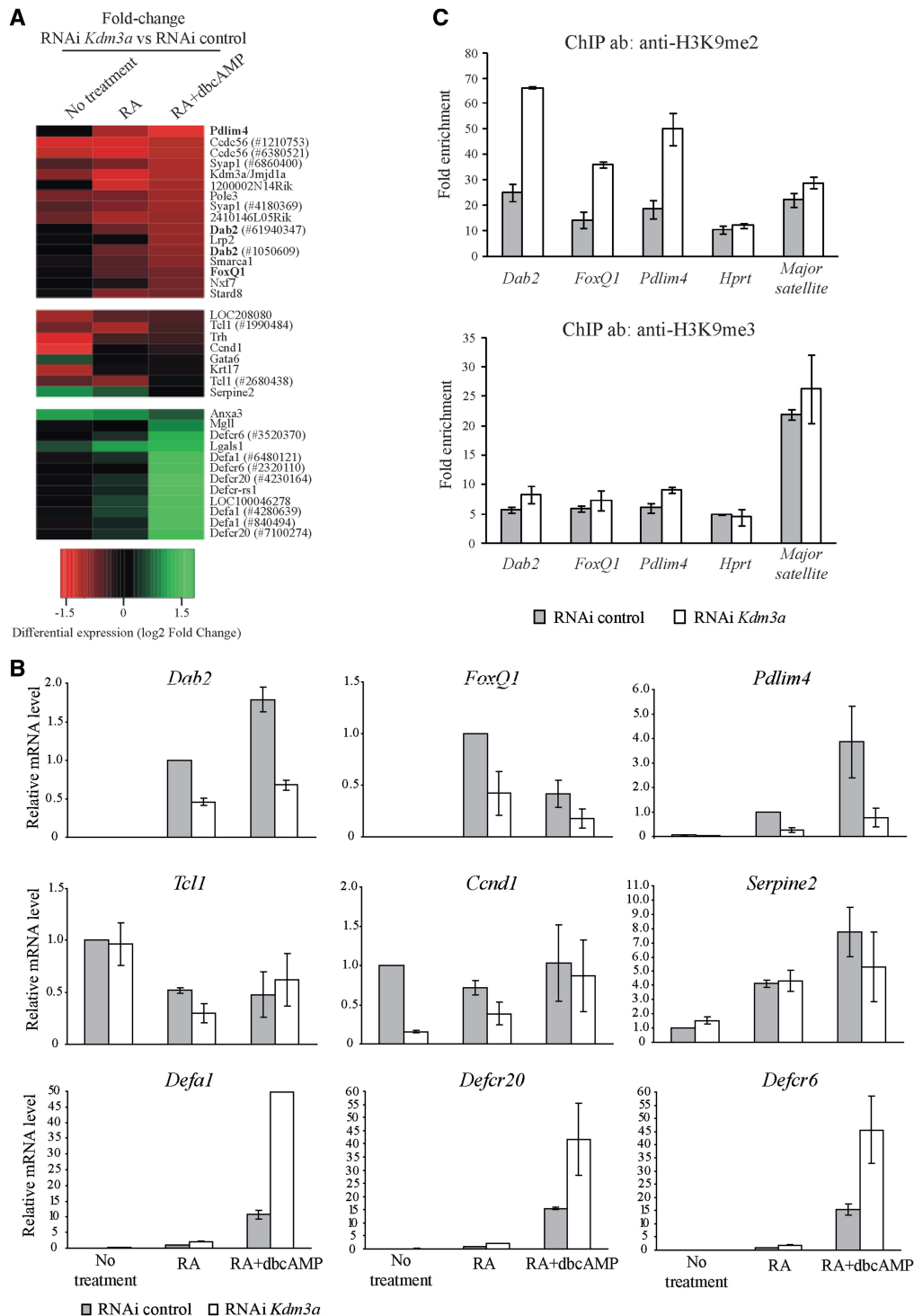
Figure 3. Kdm3a positively regulates the expression of *Dab2*, *FoxQ1* and *Pdlim4* and this correlates with their H3K9me2 demethylation. (**A**) Heatmap depicting microarray expression changes (log$_2$) of selected differentiation-associated genes after *Kdm3a*-knockdown in F9 cells after RA and RA+dbcAMP treatment. Differential gene expression was calculated between RNAi control F9 cells and RNAi *Kdm3a* cells for each time-point separately (no treatment, RA and RA+dbcAMP). Genes were ordered from the most down-regulated to the most up-regulated according to their expression changes upon *Kdm3a*-knockdown at 6 days after RA+dbcAMP treatment. Double appearances indicate multiple microarray probes for the respective gene (probe ID in brackets). (**B**) Kdm3a positively regulates the expression of *Dab2*, *FoxQ1* and *Pdlim4*. Expression was analysed in RNAi control and RNAi *Kdm3a* F9 cells after no treatment, treatment for 3 days with RA (RA), or treatment for 3 days with RA and then for 3 additional days with RA and dbcAMP (RA+dbcAMP). RNA extracted from these cells was subjected to qRT-PCR analysis of *Dab2*, *FoxQ1*, *Pdlim4* and control genes (*Tcl1*, *Ccnd1*, *Serpine2*, *Defa1*, *Defcr20* and *Defcr6*) with gene-specific primers. *Hprt* was used as an internal control. All transcript levels were normalized to the level recorded for RA-treated RNAi control cells. Values represent means ± SEM (*n* = 3). (**C**) Analysis of H3K9me3/me2 modifications at the promoters of the *Dab2*, *FoxQ1* and *Pdlim4* genes after RA+dbcAMP treatment of the cells. ChIP-qPCR results from (RA+dbcAMP)-treated RNAi control cells are indicated by filled bars, those from RNAi *Kdm3a* F9 cells by open bars. The gene promoters analysed and the antibody used for ChIP are indicated. The normalization method used to represent the ChIP-qPCR data is fold enrichment relative to the 'no antibody' signal (*cf.* 'Materials and Methods' section). Data are represented as means ± SEM (*n* = 3).

treatment, the expression of several genes was significantly dysregulated by *Kdm3a* depletion. Among the most strongly dysregulated were the *Pdlim4, Dab2* and *FoxQ1* genes (Figure 3A and Supplementary Table 1), reported to play a role in controlling proliferation and differentiation (34–37). Interestingly, transcript-level expression of *Dab2* and *Pdlim4* was already downregulated after 3 days of RA treatment, when the cells were in the PrE differentiation state and showed no morphological anomalies (Figure 3A). To validate our microarray analysis, we performed qRT-PCR on genes showing unchanged (*Tcl1, Ccnd1* and *Serpine2*), upregulated *(Defa1, Defcr20 and Defcr6)* or downregulated (*Dab2*, *FoxQ1* and *Pdlim4*) expression on day 6 (i.e. after RA + dbcAMP treatment) in RNAi *Kdm3a* cells as compared to the control (Figure 3B). The qRT-PCR results confirmed the microarray data. As expected, *Tcl1* and *Serpine2* showed no differential expression after 6 days of differentiation, although *Serpine2* showed a slight but significant effect in undifferentiated cells, as did *Tcl1* at the PrE stage. (Figure 3B). *Ccnd1* expression showed no dysregulation after 3 or 6 days of treatment, but it did show downregulation in undifferentiated RNAi *Kdm3a* cells as compared to control cells (Figure 3B). This is consistent with the microarray data obtained for the untreated stage, where *Ccdn1* appeared as one of three downregulated genes. As for the *Defensin* genes, the only time they showed differential regulation in RNAi *Kdm3a* cells versus control cells was after RA + dbcAMP treatment, when they appeared upregulated. In the absence of RA treatment, RNAi control and RNAi *Kdm3a* cells showed little to no expression of *Dab2, FoxQ1* or *Pdlim4* (Figure 3B). RA treatment for three days was found to induce the expression of all three genes in both cell lines (Figure 3B), but the extent of induction depended on the cell genotype: for *Dab2, FoxQ1* and *Pdlim4* respectively, expression was 2.2-, 3.9- and 2.4-fold lower in the RNAi *Kdm3a* cells than in the RNAi control cells (Figure 3B). Levels of *Dab2* and *Pdlim4* transcripts increased further in both RNAi control and RNAi *Kdm3a* cells upon treatment with RA + dbcAMP, but remained lower in the latter (Figure 3B; 2.6- and 5.1-fold, respectively). *FoxQ1* expression, on the other hand, was repressed by RA + dbcAMP treatment in both RNAi control and RNAi *Kdm3a* cells. After 6 days of treatment, the level of *FoxQ1* transcripts was 3-fold lower in the latter than in the former cells (Figure 3B). Altogether, our data indicate that Kdm3a is a positive regulator of a specific set of genes in both PrE- and PE-differentiated F9 cells, and particularly of certain master players in the differentiation process.

Kdm3a regulates the expression of *Dab2*, *FoxQ1* and *Pdlim4* through demethylation of H3K9me2

To investigate the link between the demethylase activity of Kdm3a and its effect on *Dab2, Pdlim4* and *FoxQ1* transcription, we performed ChIP experiments on RNAi control and RNAi *Kdm3a* cells after RA + dbcAMP treatment, using antibodies specifically targeting either the di- or the trimethylation level of H3K9. As expected

from the demethylase specificity described for Kdm3a, we observed no difference in enrichment level for any promoter tested with the antibody targeting the H3K9me3 mark (Figure 3C, lower panel). Under these conditions, all genes tested showed an enrichment similar to that recorded for the actively transcribed *HPRT* gene and, as described in the literature, heterochromatic major satellite sequences showed a high level of enrichment (38). When an antibody targeting the H3K9me2 mark was used (Figure 3C, upper panel), the *Dab2*, *Pdlim4* and *FoxQ1* promoter regions showed 2.5-, 2.5- and 2.1-fold higher enrichment levels, respectively, in RNAi *Kdm3a* cells than in RNAi control cells. In contrast, the enrichment levels for promoter regions of the *HPRT* gene and for major satellite sequences were unaffected by *Kdm3a* depletion. Altogether, these data support a role of Kdm3a as a transcriptional coactivator of the endoderm-associated genes *Dab2*, *Pdlim4* and *FoxQ1*, exerting its effect by demethylating H3K9me2 at their promoters.

Dab2 is a downstream effector of Kdm3a in regulating F9-cell terminal differentiation

Dab2 is of particular interest, as it has been shown to play a role in mouse endoderm differentiation (35). This and our above results led us to hypothesise that Dab2 could be a downstream effector of Kdm3a in the regulation of F9-cell endodermal differentiation. If so, we would expect *Dab2* depletion in F9 cells to impair PE differentiation without affecting *Kdm3a* expression. To test this, we used the RNAi approach to generate *Dab2*-knockdown cells (henceforth called RNAi *Dab2* cells). qRT-PCR analysis confirmed the significant knockdown at RNA level throughout the differentiation process (no expression at the undifferentiated stage, expression decreased by 95% after RA treatment and by 92% after RA + dbcAMP treatment; Figure 4A, left panel). In contrast, *Kdm3a* expression was not significantly different in RNAi control and RNAi *Dab2* cells (Figure 4A, right panel). We then observed the morphology of the RNAi control and RNAi *Dab2* cells after no treatment, RA treatment, and RA + dbcAMP treatment, so as to monitor PrE and PE differentiation in these cells. At the undifferentiated stage, no morphological differences were observed between RNAi *Dab2* cells and RNAi control cells (Figure 4B). After RA treatment, both the RNAi *Dab2* cells and the RNAi control cells displayed the morphological features of PrE cells (Figure 4B). After RA + dbcAMP treatment and in contrast to the control RNAi cells, most of the RNAi *Dab2* cells retained their PrE identity, as shown by their PrE-like morphology and by expression of TROMA-1 (Figure 4B and C). In agreement with these findings, qRT-PCR analysis of TM expression revealed TM induction in RNAi control cells after RA + dbcAMP treatment, but drastically reduced TM induction in RNAi *Dab2* cells, confirming failure of the vast majority of the *Dab2* knockdown cells to differentiate into PE cells (Figure 4D). This phenotype is highly similar to what we observed in *Kdm3a* knockdown cells, indicating that *Dab2*
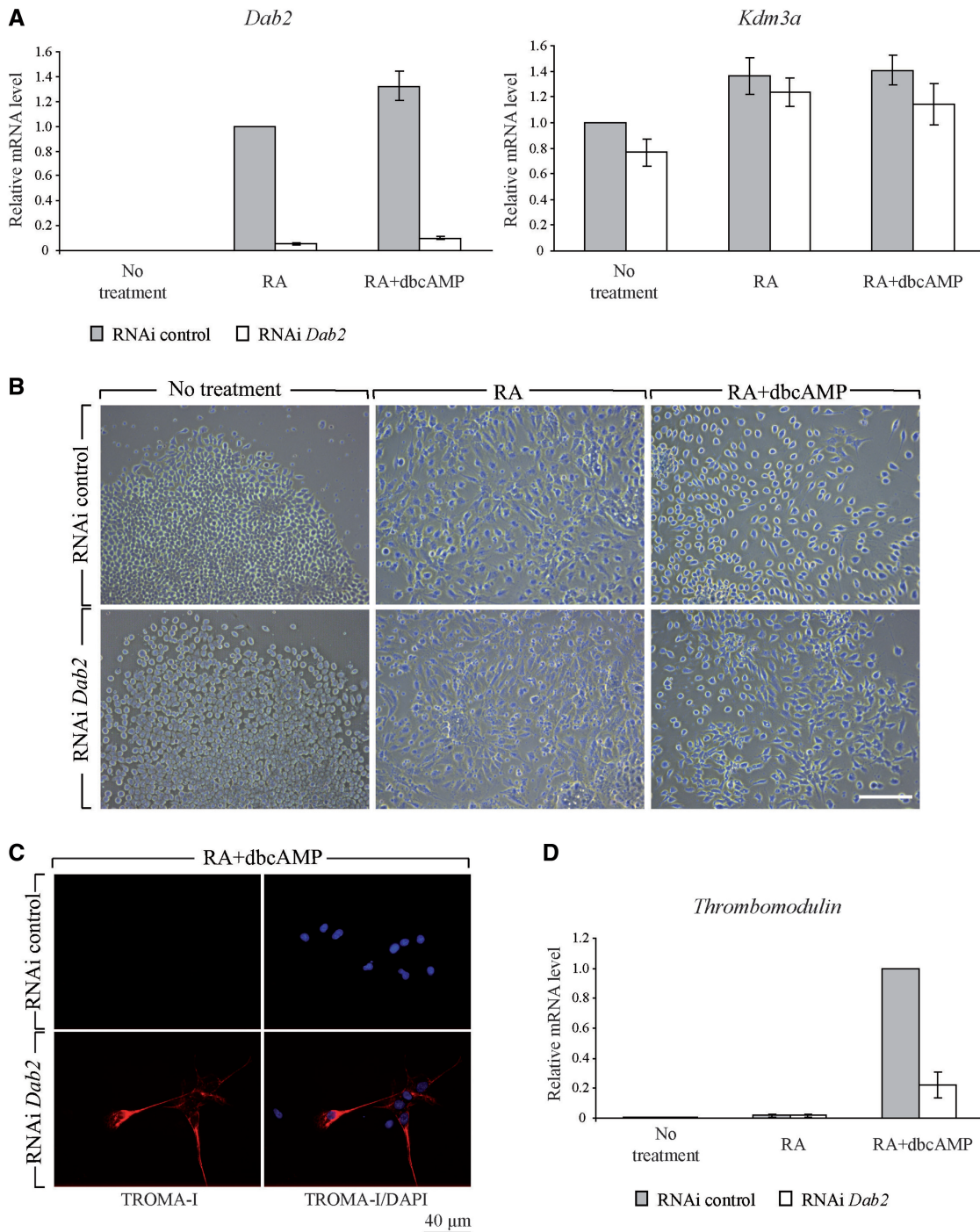
Figure 4. Dab2 is a downstream effector of Kdm3a and contributes to progression through F9-cell terminal differentiation. F9 cells were infected with the empty pRS vector (RNAi control) or the *Dab2*-targeting pRS vector (RNAi *Dab2*). After selection, RNAi control and RNAi *Dab2* F9 cells were left untreated (no treatment) or cultured with RA for 3 days (RA) or with RA for 3 days and then for 3 additional days with RA and dbcAMP (RA + dbcAMP). (**A**) Specific downregulation of *Dab2* expression in RNAi *Dab2* cells. mRNA was subjected to qRT-PCR analysis with *Dab2* (left panel) or *Kdm3a* (right panel) specific primers. All transcript levels were normalized to *Hprt* and then subtracted from the level recorded for RA-treated RNAi control cells. Data are presented as means ± SEM ($n = 5$). (**B**) Dab2 is required for PE differentiation of F9 cells. RNAi *Dab2* and RNAi control cells show similar morphology after RA treatment. But, RNAi *Dab2* cells fail to complete terminal differentiation into PE cells upon RA + dbcAMP treatment. Cells were photographed under a phase contrast microscope. Bar = 200 μm. (**C**) RNAi *Dab2* F9 cells still express TROMA-1 after RA + dbcAMP treatment. Immunofluorescence detection of TROMA-1 was performed on RNAi control and RNAi *Dab2* F9 cells cultured on glass cover slips and treated for 6 days with RA + dbcAMP. Cytoplasmic TROMA-1 staining is absent, as expected, in RNAi control cells fully differentiated into PE cells, but still present in RNAi *Dab2* cells having failed to complete PE differentiation and still at the PrE differentiation stage. Cell DNA content was visualized by DAPI staining. Bar = 40 μm. (**D**) Downregulation of expression of the PE differentiation marker *Thrombomodulin* (TM) in RNAi *Dab2* cells compared to RNAi control cells. Cells were either not treated (no treatment), treated for 3 days with RA (RA), or treated for 3 days with RA and then for 3 additional days with RA and dbcAMP (RA + dbcAMP). Their mRNA was analysed by qRT-PCR. *Hprt* was used as an internal control. All transcript levels were corrected by the normalized level recorded for (RA + dbcAMP)-treated RNAi control cells. Values represent means ± SEM ($n = 5$).

depletion, like *Kdm3a* depletion, prevents the cells from fully differentiating into PE cells after RA + dbcAMP treatment. Both *Dab2* and *Kdm3a* are thus required for complete PE differentiation, but *Dab2* is not required for normal *Kdm3a* expression. This suggests that *Dab2* might indeed be a downstream effector of *Kdm3a* in the regulation of F9-cell terminal differentiation.

To test this hypothesis, we investigated whether over-expression of *Dab2* in RNAi *Kdm3a* cells might restore complete PE differentiation. Not knowing at which step of the differentiation process Dab2 might be crucial to achieving terminal differentiation, we transfected RNAi *Kdm3a* cells with a plasmid expressing *Dab2* cDNA or with a control plasmid at different time points during the differentiation process: on Day 2, 3 or 4 or on Days 2 and 4 (Figure 5A). After 6 days of treatment (3 days with RA plus 3 additional days with RA + dbcAMP), *Dab2* was significantly over-expressed whatever the transfection schedule, but its expression was highest in cells transfected on both Day 2 and 4 (Figure 5B). The ability of these cell lines to undergo PE differentiation was analysed after 6 days of treatment. Whether they expressed *Dab2* or not and whatever the transfection vector or schedule, RNAi *Kdm3a* cells showed incomplete PE differentiation, as demonstrated by both morphological analysis (Figure 5C) and transcript-level *Thrombomodulin* expression (Figure 5D). In the TM expression assays, RNAi control cells (Figure 5D) always showed significantly higher TM transcript levels than RNAi *Kdm3a* cells, whether the latter were non-transfected, control-transfected or *Dab2*-transfected. Moreover, no significant difference in TM expression appeared among these variously treated RNAi *Kdm3a* cells, although twice-transfected cells did show a slightly lower TM transcript level than once-transfected cells, whether they expressed *Dab2* or not. This (non-significant) effect would thus appear to be linked to repeat transfection. To understand why *Dab2* over-expression does not restore the PE phenotype in RNAi *Kdm3a* cells, we analysed the expression of *FoxQ1* and *Pdlim4*, the two other master players in the differentiation process found to be dysregulated in RNAi *Kdm3a* cells. qRT-PCR analysis revealed significantly lower expression of both genes in *Dab2*-transfected RNAi *Kdm3a* cells than in RNAi control cells, and the extent of reduction was similar to that observed in non-transfected RNAi *Kdm3a* cells (Figure 5E). Thus, *Dab2* over-expression cannot restore *FoxQ1* and *Pdlim4* expression in *Kdm3a*-knockdown cells. Hence, *Dab2* appears to be necessary for endoderm differentiation but not sufficient to promote F9-cell terminal differentiation when *Kdm3a* is absent.

Altogether, our results suggest that Kdm3a controls F9-cell terminal differentiation by regulating the expression of a set of endoderm master players such as *Dab2*, *FoxQ1* and *Pdlim4*. Furthermore, all of these genes appear to be necessary to enable F9 cells to complete their terminal differentiation into PE cells.

DISCUSSION

Epigenetic mechanisms, such as histone methylation, are an integral part of gene expression regulatory mechanisms. Molecular studies have revealed an increasing number of histone-modifying enzymes (e.g. histone methyltransferases and demethylases), and biochemical assays have enabled investigators to characterise their substrates. Now a key challenge is to understand which biological and developmental processes are regulated by these enzymes.

Several studies suggest an involvement of histone demethylases in cell differentiation. Kdm4c has been demonstrated to act as a positive regulator of the key pluripotency transcription factor *Nanog*, presumably by removing H3K9 methylation at the promoter of this gene (18). Enzymes of the Kdm5 and Kdm6 groups are reported to have specific roles in regulating H3K4 and H3K27 methylation, respectively, at developmentally regulated genes (39–42). Here, using F9 mouse embryonal carcinoma cells as a convenient model for studying crucial events in early endodermal differentiation, we have explored the role of the H3K9me2-specific histone demethylase Kdm3a in this differentiation process. Our results indicate that Kdm3a contributes to deciding cell fate through its ability to regulate genes encoding master players in the differentiation process.

We show that knockdown of *Kdm3a* does not affect the capacity of F9 cells to morphologically differentiate into PrE cells, but largely abolishes their ability to differentiate into PE cells. Kdm3a is thus not essential to initiating differentiation, but required at a later stage for terminal differentiation. We further show that in F9 cells stimulated to undergo terminal differentiation (by RA + dbcAMP treatment), Kdm3a regulates the H3K9 dimethylation status at the promoters of three genes encoding regulators of differentiation: *Dab2, Pdlim4* and *FoxQ1*. Increased H3K9 dimethylation at these promoters in RNAi *Kdm3a* cells correlates with reduced expression, strongly suggesting that Kdm3a positively regulates the expression of these genes through its demethylase activity.

We have thus identified a new role for Kdm3a: controlling the epigenetic state of regulator genes during differentiation. It appears that expression of *Dab2* and *Pdlim4* is downregulated already at the PrE stage in *Kdm3a*-depleted cells, whereas expression of two other endoderm-associated genes (*Gata6*, *Hnf4a*) and two RA-associated genes (*Rxrα*, *Lamb1*) is not altered. In keeping with the morphologically normal differentiation of RNAi *Kdm3a* cells into PrE cells, this suggests that the histone demethylase Kdm3a does not regulate globally the response of F9 cells to RA, but rather plays a role in regulating a set of genes whose expression enables cells to acquire the competence to further differentiate into PE cells. *Dab2*, shown to play a role in endoderm formation during early mouse embryogenesis (35), is of particular interest in this respect. *Dab2*-knockout mice develop normally up to the blastocyst stage, but fail to develop beyond E6.5 because of a defective extra-embryonic visceral endoderm. This means that Dab2 is not essential for primitive endoderm differentiation but rather for
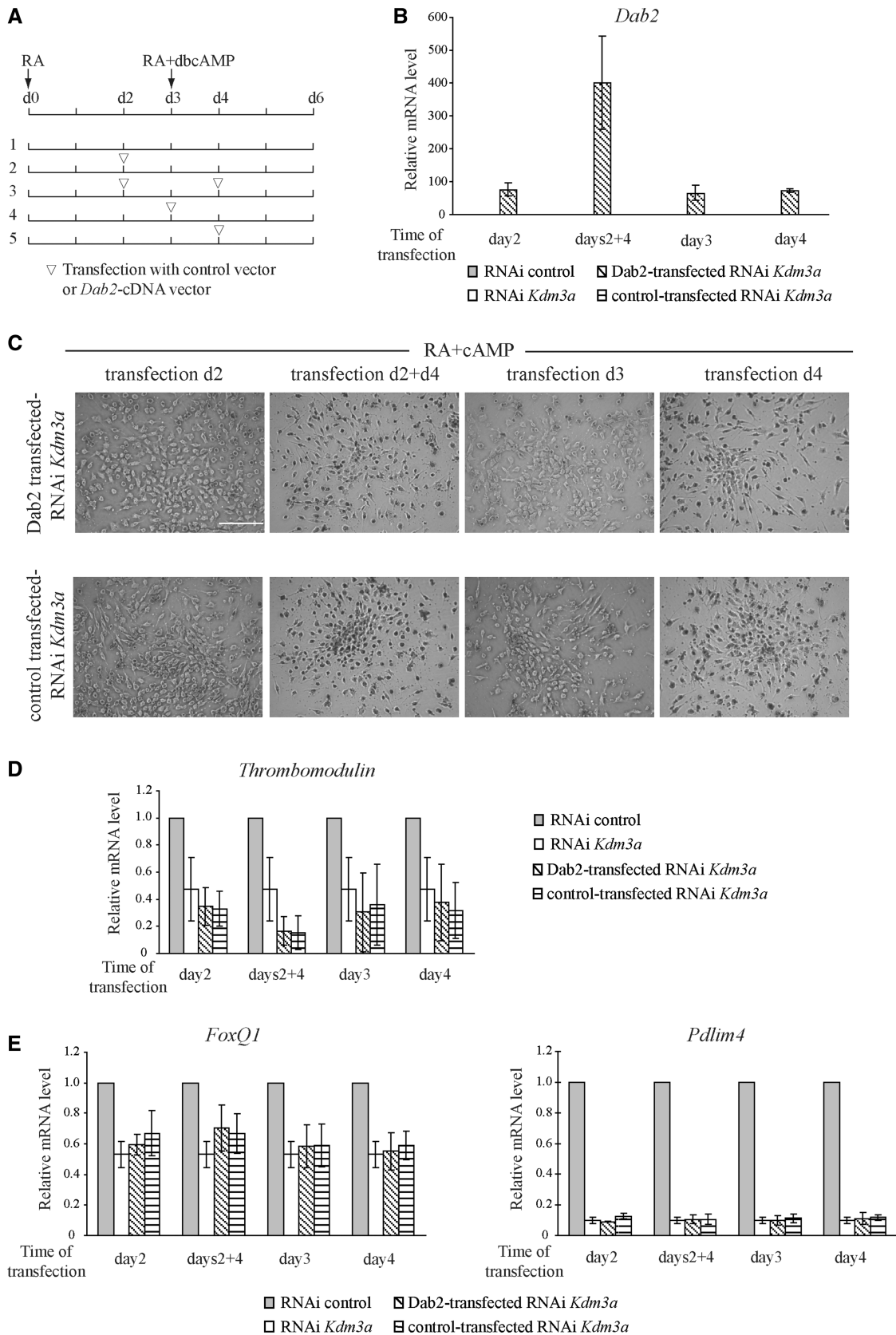
Figure 5. *Dab2* over-expression alone is insufficient to restore a normal phenotype in RNAi *Kdm3a* cells. (**A**) Schematic representation of the transfection schedule applied during the F9-cell differentiation process. RNAi *Kdm3a* cells were either untransfected (timeline #1) or transfected with a *Dab2* expression plasmid or a control vector at different times during the differentiation process: after 2 days of RA treatment (#2), at the start of dbcAMP treatment after 3 days of RA treatment(#4), after 4 days of treatment (#5; i.e. after 3 days of RA treatment and 1 day of

(continued)

progression through extra-embryonic endoderm differentiation (35). Interestingly, we show that knockdown of *Dab2* in F9 cells mimics the *Kdm3a*-knockdown phenotype without affecting *Kdm3a* expression, confirming the need of *Dab2* expression for endoderm differentiation. Yet ectopic over-expression of *Dab2* in RNAi *Kdm3a* cells does not restore the ability of these cells to differentiate into PE cells, suggesting that *Dab2* alone is not sufficient to promote complete PE differentiation. This may be due to the fact that levels of *Pdlim4* and *FoxQ1,* two other master players in the differentiation process, remain lower in RNAi *Kdm3a* cells than in control cells. We therefore suggest that Dab2 is necessary but, on its own, insufficient to promote complete terminal differentiation of F9 cells. We propose that PE terminal differentiation results from concerted action of a set of genes whose regulation is controlled by the histone demethylase Kdm3a.

It is noteworthy that *Kdm3a* knockout, in contrast to *Dab2* knockout, does not lead to embryonic lethality in mice. *Kdm3a*$^{-/-}$ embryos develop normally, and only in adulthood do they show anomalies (obesity and hyperlipidemia) (17). Various explanations might be proposed for this apparent contradiction between the *in vivo* and *in vitro* effects of a Kdm3a deficiency. First, maternal *Kdm3a* transcripts might contribute to the development of the embryo, at least up to the gastrulation stage. Secondly, other histone demethylases might compensate *in vivo* for the lack of Kdm3a, enabling the embryo to pass a crucial developmental step during embryogenesis. Finally, we cannot exclude the possibility that the involvement of Kdm3a in differentiation might be restricted to F9 embryonal carcinoma cells. Although we cannot rule out any of these hypotheses, it seems unlikely that the role of Kdm3a in cell fate decision is limited to F9 cells, especially in the light of previous work suggesting a role of Kdm3a in cell fate decision in early development: Kdm3a-mediated demethylation of H3K9me2 at promoters of pluripotency-associated genes is involved in the self-renewal of ES cells (18). The present results contribute to our understanding of histone demethylase functions and enable us to propose a new role for Kdm3a in terminal endoderm differentiation, as a key modulator of cell fate decision.

In summary, our study highlights the importance of histone demethylases in development and cell differentiation, in the wake of findings on Kdm4c, Kdm5d and Kdm6a (see above). We show that in correlation with H3K9 demethylation, Kdm3a positively regulates the endoderm markers *Dab2*, *Pdlim4* and *FoxQ1* to allow terminal differentiation. In other words, our findings enable us to propose a new role for Kdm3a in terminal endoderm differentiation, as a key modulator of cell fate decision. Further studies may reveal an involvement of Kdm3a in yet other differentiation pathways.

SUPPLEMENTARY DATA

Supplementary Data are available at NAR Online: Supplementary Tables 1 and 2 and Supplementary Figures 1–3.

FUNDING

REFERENCES

1. Mohn,F. and Schubeler,D. (2009) Genetics and epigenetics: stability and plasticity during cellular differentiation. *Trends Genet.*, **25**, 129–136.
2. Christophersen,N.S. and Helin,K. (2010) Epigenetic control of embryonic stem cell fate. *J. Exp. Med.*, **207**, 2287–2295.
3. Bernstein,B.E., Mikkelsen,T.S., Xie,X., Kamal,M., Huebert,D.J., Cuff,J., Fry,B., Meissner,A., Wernig,M., Plath,K. *et al.* (2006) A bivalent chromatin structure marks key developmental genes in embryonic stem cells. *Cell*, **125**, 315–326.
4. Fisher,C.L. and Fisher,A.G. (2011) Chromatin states in pluripotent, differentiated, and reprogrammed cells. *Curr. Opin. Genet. Dev.*, **21**, 140–146.
5. Mattout,A. and Meshorer,E. (2010) Chromatin plasticity and genome organization in pluripotent embryonic stem cells. *Curr. Opin. Cell Biol.*, **22**, 334–341.
6. Meissner,A. (2010) Epigenetic modifications in pluripotent and differentiated cells. *Nat. Biotechnol.*, **28**, 1079–1088.
7. Shi,Y., Lan,F., Matson,C., Mulligan,P., Whetstine,J.R., Cole,P.A. and Casero,R.A. (2004) Histone demethylation mediated by the nuclear amine oxidase homolog LSD1. *Cell*, **119**, 941–953.

Figure 5. Continued

RA + dbcAMP treatment), once on day 2 and again on day 4 of the protocol (#3). (**B**) *Dab2* is well over-expressed after transfection. At the end of the differentiation process, *Dab2* over-expression was analysed by qRT-PCR. *Hprt* was used as internal control. All transcript levels are normalized with respect to the level recorded for (RA + dbcAMP)-treated RNAi control cells. Values are means ± SEM ($n = 3$). (**C**) *Dab2*-transfected RNAi *Kdm3a* cells showed incomplete PE differentiation. RNAi *Kdm3a* cells treated with RA for 3 days and then for 3 more days with RA + dbcAMP were transfected with a plasmid expressing *Dab2* cDNA or a control expression plasmid at the indicated time(s) during the differentiation process and photographed under a phase contrast microscope. RNAi *Kdm3a* cells transfected with control plasmid kept a PrE morphology (lower panels) similar to that observed for untransfected RNAi *Kdm3a* cells. *Dab2*-transfected RNAi *Kdm3a* (upper panels) cells did not display a fully differentiated parietal endoderm morphology. Bar = 200 μm. (**D**) Significant downregulation of expression of the PE differentiation marker *Thrombomodulin* (TM) in *Dab2*-transfected RNAi *Kdm3a* cells. RNAi control and RNAi *Kdm3*a cells were treated for 3 days with RA and then for 3 days with RA + dbcAMP. RNAi *Kdm3a* cells were transfected or not with a control or *Dab2* expression plasmid at the indicated time(s) during the differentiation process. Isolated RNA was analysed by qRT-PCR. *Hprt* was used as an internal control. All transcript levels were normalized with respect to the level recorded for (RA + dbcAMP)-treated RNAi control cells. Values are means ± SEM ($n = 3$). (**E**) Expression of *FoxQ1* and *Pdim4* is downregulated in *Dab2*-transfected RNAi *Kdm3a* cells. RNAi *Kdm3a* cells, untransfected or transfected with a control or *Dab2* expression plasmid, and RNAi control cells were treated with RA for 3 days and then for 3 additional days with RA + dbcAMP. Relative transcript-level expression of the *FoxQ1* and *Pdlim4* genes was analysed by qRT-PCR. *Hprt* was used as an internal control. All transcript levels were normalized with respect to the level recorded for (RA + dbcAMP)-treated RNAi control cells. Values are means ± SEM ($n = 3$).

8. Tsukada,Y., Fang,J., Erdjument-Bromage,H., Warren,M.E., Borchers,C.H., Tempst,P. and Zhang,Y. (2006) Histone demethylation by a family of JmjC domain-containing proteins. *Nature*, **439**, 811–816.

9. Pedersen,M.T. and Helin,K. (2010) Histone demethylases in development and disease. *Trends Cell Biol.*, **20**, 662–671.

10. Jenuwein,T. (2006) The epigenetic magic of histone lysine methylation. *FEBS J.*, **273**, 3121–3135.

11. Tachibana,M., Sugimoto,K., Nozaki,M., Ueda,J., Ohta,T., Ohki,M., Fukuda,M., Takeda,N., Niida,H., Kato,H. *et al.* (2002) G9a histone methyltransferase plays a dominant role in euchromatic histone H3 lysine 9 methylation and is essential for early embryogenesis. *Genes Dev.*, **16**, 1779–1791.

12. Fodor,B.D., Kubicek,S., Yonezawa,M., O'Sullivan,R.J., Sengupta,R., Perez-Burgos,L., Opravil,S., Mechtler,K., Schotta,G. and Jenuwein,T. (2006) Jmjd2b antagonizes H3K9 trimethylation at pericentric heterochromatin in mammalian cells. *Genes Dev.*, **20**, 1557–1562.

13. Wissmann,M., Yin,N., Muller,J.M., Greschik,H., Fodor,B.D., Jenuwein,T., Vogler,C., Schneider,R., Gunther,T., Buettner,R. *et al.* (2007) Cooperative demethylation by JMJD2C and LSD1 promotes androgen receptor-dependent gene expression. *Nat. Cell Biol.*, **9**, 347–353.

14. Yamane,K., Toumazou,C., Tsukada,Y., Erdjument-Bromage,H., Tempst,P., Wong,J. and Zhang,Y. (2006) JHDM2A, a JmjC-containing H3K9 demethylase, facilitates transcription activation by androgen receptor. *Cell*, **125**, 483–495.

15. Saccani,S. and Natoli,G. (2002) Dynamic changes in histone H3 Lys 9 methylation occurring at tightly regulated inducible inflammatory genes. *Genes Dev.*, **16**, 2219–2224.

16. Okada,Y., Scott,G., Ray,M.K., Mishina,Y. and Zhang,Y. (2007) Histone demethylase JHDM2A is critical for Tnp1 and Prm1 transcription and spermatogenesis. *Nature*, **450**, 119–123.

17. Tateishi,K., Okada,Y., Kallin,E.M. and Zhang,Y. (2009) Role of Jhdm2a in regulating metabolic gene expression and obesity resistance. *Nature*, **458**, 757–761.

18. Loh,Y.H., Zhang,W., Chen,X., George,J. and Ng,H.H. (2007) Jmjd1a and Jmjd2c histone H3 Lys 9 demethylases regulate self-renewal in embryonic stem cells. *Genes Dev.*, **21**, 2545–2557.

19. Krieg,A.J., Rankin,E.B., Chan,D., Razorenova,O., Fernandez,S. and Giaccia,A.J. (2010) Regulation of the histone demethylase JMJD1A by hypoxia-inducible factor 1 alpha enhances hypoxic gene expression and tumor growth. *Mol. Cell Biol.*, **30**, 344–353.

20. Lehtonen,E., Laasonen,A. and Tienari,J. (1989) Teratocarcinoma stem cells as a model for differentiation in the mouse embryo. *Int. J. Dev. Biol.*, **33**, 105–115.

21. Strickland,S., Smith,K.K. and Marotti,K.R. (1980) Hormonal induction of differentiation in teratocarcinoma stem cells: generation of parietal endoderm by retinoic acid and dibutyryl cAMP. *Cell*, **21**, 347–355.

22. Strickland,S. and Mahdavi,V. (1978) The induction of differentiation in teratocarcinoma stem cells by retinoic acid. *Cell*, **15**, 393–403.

23. Chahrour,M., Jung,S.Y., Shaw,C., Zhou,X., Wong,S.T., Qin,J. and Zoghbi,H.Y. (2008) MeCP2, a key contributor to neurological disease, activates and represses transcription. *Science*, **320**, 1224–1229.

24. Metivier,R., Penot,G., Hubner,M.R., Reid,G., Brand,H., Kos,M. and Gannon,F. (2003) Estrogen receptor-alpha directs ordered, cyclical, and combinatorial recruitment of cofactors on a natural target promoter. *Cell*, **115**, 751–763.

25. Fuks,F., Burgers,W.A., Brehm,A., Hughes-Davies,L. and Kouzarides,T. (2000) DNA methyltransferase Dnmt1 associates with histone deacetylase activity. *Nat. Genet.*, **24**, 88–91.

26. Brummelkamp,T.R., Bernards,R. and Agami,R. (2002) A system for stable expression of short interfering RNAs in mammalian cells. *Science*, **296**, 550–553.

27. Kemler,R., Brulet,P., Schnebelen,M.T., Gaillard,J. and Jacob,F. (1981) Reactivity of monoclonal antibodies against intermediate filament proteins during embryonic development. *J. Embryol. Exp. Morphol.*, **64**, 45–60.

28. Verheijen,M.H., Wolthuis,R.M., Bos,J.L. and Defize,L.H. (1999) The Ras/Erk pathway induces primitive endoderm but prevents parietal endoderm differentiation of F9 embryonal carcinoma cells. *J. Biol. Chem.*, **274**, 1487–1494.

29. Li,C. and Gudas,L.J. (1996) Murine laminin B1 gene regulation during the retinoic acid- and dibutyryl cyclic AMP-induced differentiation of embryonic F9 teratocarcinoma stem cells. *J. Biol. Chem.*, **271**, 6810–6818.

30. Wan,Y.J., Wang,L. and Wu,T.C. (1994) The expression of retinoid X receptor genes is regulated by all-trans- and 9-cis-retinoic acid in F9 teratocarcinoma cells. *Exp. Cell Res.*, **210**, 56–61.

31. Taneja,R., Bouillet,P., Boylan,J.F., Gaub,M.P., Roy,B., Gudas,L.J. and Chambon,P. (1995) Reexpression of retinoic acid receptor (RAR) gamma or overexpression of RAR alpha or RAR beta in RAR gamma-null F9 cells reveals a partial functional redundancy between the three RAR types. *Proc. Natl Acad. Sci. USA*, **92**, 7854–7858.

32. Morrisey,E.E., Tang,Z., Sigrist,K., Lu,M.M., Jiang,F., Ip,H.S. and Parmacek,M.S. (1998) GATA6 regulates HNF4 and is required for differentiation of visceral endoderm in the mouse embryo. *Genes Dev.*, **12**, 3579–3590.

33. Weiler-Guettler,H., Yu,K., Soff,G., Gudas,L.J. and Rosenberg,R.D. (1992) Thrombomodulin gene regulation by cAMP and retinoic acid in F9 embryonal carcinoma cells. *Proc. Natl Acad. Sci. USA*, **89**, 2155–2159.

34. Hong,H.K., Noveroske,J.K., Headon,D.J., Liu,T., Sy,M.S., Justice,M.J. and Chakravarti,A. (2001) The winged helix/forkhead transcription factor Foxq1 regulates differentiation of hair in satin mice. *Genesis*, **29**, 163–171.

35. Yang,D.H., Smith,E.R., Roland,I.H., Sheng,Z., He,J., Martin,W.D., Hamilton,T.C., Lambeth,J.D. and Xu,X.X. (2002) Disabled-2 is essential for endodermal cell positioning and structure formation during mouse embryogenesis. *Dev. Biol.*, **251**, 27–44.

36. Vanaja,D.K., Grossmann,M.E., Cheville,J.C., Gazi,M.H., Gong,A., Zhang,J.S., Ajtai,K., Burghardt,T.P. and Young,C.Y. (2009) PDLIM4, an actin binding protein, suppresses prostate cancer cell growth. *Cancer Invest.*, **27**, 264–272.

37. Feuerborn,A., Srivastava,P.K., Kuffer,S., Grandy,W.A., Sijmonsma,T.P., Gretz,N., Brors,B. and Grone,H.J. (2011) The Forkhead factor FoxQ1 influences epithelial differentiation. *J. Cell Physiol.*, **226**, 710–719.

38. Rosenfeld,J.A., Wang,Z., Schones,D.E., Zhao,K., DeSalle,R. and Zhang,M.Q. (2009) Determination of enriched histone modifications in non-genic portions of the human genome. *BMC Genomics*, **10**, 143.

39. Agger,K., Cloos,P.A., Christensen,J., Pasini,D., Rose,S., Rappsilber,J., Issaeva,I., Canaani,E., Salcini,A.E. and Helin,K. (2007) UTX and JMJD3 are histone H3K27 demethylases involved in HOX gene regulation and development. *Nature*, **449**, 731–734.

40. Akimoto,C., Kitagawa,H., Matsumoto,T. and Kato,S. (2008) Spermatogenesis-specific association of SMCY and MSH5. *Genes Cells*, **13**, 623–633.

41. De Santa,F., Totaro,M.G., Prosperini,E., Notarbartolo,S., Testa,G. and Natoli,G. (2007) The histone H3 lysine-27 demethylase Jmjd3 links inflammation to inhibition of polycomb-mediated gene silencing. *Cell*, **130**, 1083–1094.

42. Iwase,S., Lan,F., Bayliss,P., de la Torre-Ubieta,L., Huarte,M., Qi,H.H., Whetstine,J.R., Bonni,A., Roberts,T.M. and Shi,Y. (2007) The X-linked mental retardation gene SMCX/JARID1C defines a family of histone H3 lysine 4 demethylases. *Cell*, **128**, 1077–1088.